A Low-Profile Dual-Polarized Substrate Integrated Magneto-Electric Dipole MIMO Antenna

Mu-Sheng Liang, Ye Zhou, Xue-Song Yang, *Senior Member, IEEE*, and Pei-Fang Wu

***Abstract*—A magneto-electric dipole (MED) multiple-input–multiple-output (MIMO) antenna with low-profile, dual-polarized, and substrate integrated properties is proposed. The antenna element is composed of four fan-shaped patches lying on the radiation plane and four vertical metal vias linking the patches and the ground. Compared with the common MED antennas, the proposed MED antenna element has a lower profile of 0.1λ. Besides, it is fed by microstrip lines via two orthogonal H-shaped slots, resulting in a broad impedance bandwidth of 40% (3–4.5 GHz) and a steady gain in the entire operational band. The ports isolation is higher than 27 dB, the cross-polarization discrimination is higher than 37 dB, and the measured radiation efficiency is greater than 70%. Furthermore, four antenna elements are utilized to form a MIMO antenna, which can obtain better ports isolation characteristics under the condition that the element spacing is half wavelength. Finally, the MIMO antenna is simulated, fabricated and measured. The results verify the rationality of the design.**

***Index Terms*—Dual-polarization, low-profile, magneto-electric dipole (MED), multiple-input–multiple-output (MIMO), substrate integrated.**

I. Introduction

WITH the rapid development of wireless communication technology today, people have higher and higher requirements for data transmission quality and speed. By using the complementary antenna principle [1], magneto-electric dipole (MED) antenna has excellent electromagnetic properties, such as wide frequency band, almost the same radiation pattern of E-plane, and H-plane. It is especially suitable to be used as a base-station antenna.

In order to miniaturize the system, realizing a low-profile and miniaturized MED antenna becomes a choice. Generally, an MED antenna is composed of a half-wavelength electric dipole and two quarter-wavelength vertical short-circuit patches [2]. Therefore, increasing the current path of the vertical shorting patch can reduce the profile of the antenna. Many methods have been utilized to achieve the miniaturization of the antenna. For example, the equivalent magnetic dipole short-circuit patch is folded [3], [4], a metamaterial is loaded between two vertical short-circuit patches [5], or the MED antenna is designed by means of substrate integration [6], [7], [8], [9], [10], [11].

Compared with single-polarized antennas, dual-polarized antennas can transmit multiple signals at the same time, thus helping to reduce the number of antennas, cut costs, and improve diversity gain. However, when designing a dual-polarized MED antenna or array [12], [13], [14], [15], [16], due to the mutual influence of the two polarizations, it is difficult to reduce the cross-section height by folding the shorting pieces. Therefore, how to reduce the antenna profile is a key problem to be solved urgently in the design of miniaturized dual-polarized MED antenna.

In this letter, a broadband low-profile dual-polarized dielectric integrated MED multiple-input–multiple-output (MIMO) antenna is designed by using multilayer dielectric integration and microstrip slot coupling feeding technologies. The antenna element structure in this design is different from the traditional dual-polarized MED antenna. When the antenna element works in the operational mode of the electric dipole, the four radiating patches work together. In other words, it reduces the size of the antenna because the relative permittivity of the dielectric substrate is greater than that of air. The profile of the antenna element becomes much lower in a broad impedance band. Moreover, a four-element $\pm 45^\circ$ dual-polarized MIMO antenna composed of the proposed MED antenna element is presented. The simulation analysis is carried out first, and then the MIMO antenna is fabricated and measured. Desired results are obtained over a wide operational band at last.

II. Antenna Element

A. Geometry

The structure and feeding network of the $\pm 45^\circ$ dual-polarized MED antenna element proposed in this letter are shown in Fig. 1. The antenna consists of two dielectric substrates with the same physical dimension. The relative dielectric constants of the upper and lower dielectrics are 2.2 and 3.55, respectively. The loss tangents are 0.0009 and 0.0027, and the thicknesses are 8.0 and 0.5 mm, respectively. The electrical dimensions of the antenna element are $0.58\lambda_0 \times 0.58\lambda_0 \times 0.1\lambda_0$ (λ_0 is the free-space wavelength at 3.75 GHz). Detailed dimensions are summarized in Table I.

The radiating structure of the antenna element consists of two pairs of fan-shaped radiating patches on the upper layer of the first dielectric substrate, and four short-circuit vias connecting the patches and the ground.

The radiating patches constitute electric dipoles, and the gaps between the patches are equivalent to magnetic dipoles,

Manuscript received 8 December 2022; revised 16 January 2023; accepted 7 February 2023. Date of publication 10 February 2023; date of current version 2 June 2023. This work was supported in part by the National Natural Science Foundation of China under Grant 61731005 and Grant 62271112; and in part by the Applied Foundational Research Project of Sichuan Province under Grant 2021YJ0100. *(Corresponding author: Xue-Song Yang.)*

Mu-Sheng Liang and Xue-Song Yang are with the Institute of Applied Physics, University of Electronic Science and Technology of China, Chengdu 611731, China, and also with the Yangtze Delta Region Institute (Huzhou), University of Electronic Science and Technology of China, Huzhou 313001, China (e-mail: msliang@uestc.edu.cn; xsyang@uestc.edu.cn).

Ye Zhou and Pei-Fang Wu are with the Institute of Applied Physics, University of Electronic Science and Technology of China, Chengdu 611731, China (e-mail: 1144529370@qq.com; 785367719@qq.com).

Digital Object Identifier 10.1109/LAWP.2023.3244031

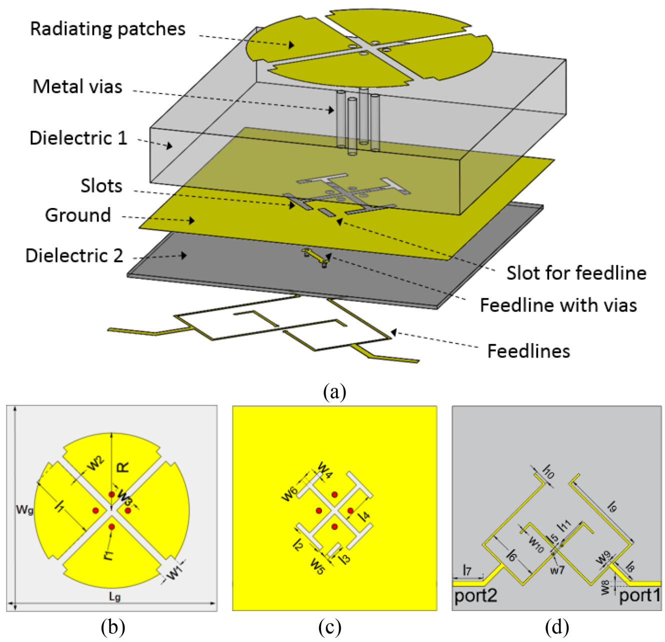

Fig. 1. Geometry of the proposed MED antenna element. (a) Exploded view. (b) Top view of the first dielectric substrate. (c) Bottom view of the first dielectric substrate. (d) Bottom view of the second dielectric substrate.

TABLE I
DIMENSIONS OF THE MED ANTENNA ELEMENT (UNIT: mm)

Parameter	Value	Parameter	Value	Parameter	Value
Lg	46	*l7*	7.13	*w4*	1
Wg	46	*l8*	5.49	*w5*	1
l1	15.25	*l9*	19	*w6*	1
l2	7.6	*l10*	3.2	*w7* & *w10*	0.4
l3	3.6	*l11*	6.76	*w8*	1.1
l4	7	*w1*	4.5	*w9*	1
l5	2.13	*w2*	1.5	*R*	17
l6	12	*w3*	5	*r1*	0.6

and the two constitute complementary radiating antennas. Two fork-shaped power dividers printed on the bottom surface of the lower dielectric substrate excite the upper patches through two orthogonal H-shaped slots etched in the ground between two substrates. The slots in the ground are arranged parallel to the gaps between the radiating patches, and the branch lines of the fork dividers are parallel to the slots in the ground, as depicted in Fig. 1(b). To avoid intersections between two feedlines, one feedline is cutoff and connecting with two vias to the short feedline on the upper surface of the substrate, as shown in Fig. 1(a) and (d), respectively. Meanwhile, as seen in Fig. 1(c), a slightly bigger slot is etched in the ground to place the feedline to prevent it from connecting to the metal ground.

B. Operational Principle

In order to understand the operational mechanism of the proposed MED antenna element, Fig. 2 shows the current distributions on the main radiating patches for one cycle when the element is fed at port 1 [see ports definition in Fig. 1(d)]. It can be observed that when $t = 0$ and $t = \mathrm{T}/2$, the entire

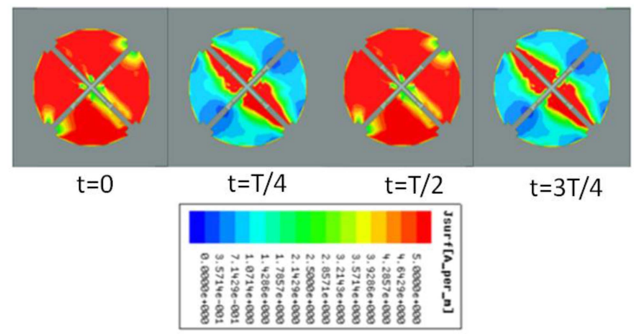

Fig. 2. Current distributions of radiating patches excited by port 1 of the MED antenna element.

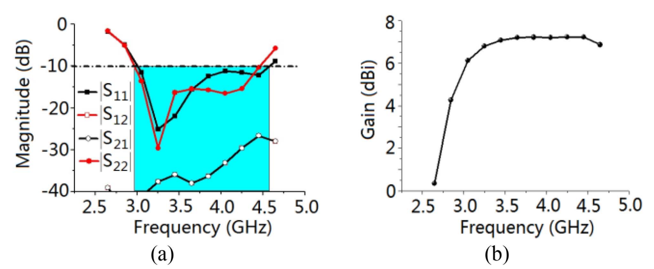

Fig. 3. Scattering parameters and gains of dual-polarized MED antenna element. (a) *S*-parameters. (b) Gains.

radiating patches work as an electric dipole. When $t = \mathrm{T}/4$ and $t = 3\mathrm{T}/4$, the currents around the gap in the $-45°$ direction are very strong, which is equivalent to the working situation of a magnetic dipole. The phase difference between the electric dipole and the magnetic dipole is exactly 90°, which realizes the complementary characteristics of the MED antenna element. It can be seen that the currents on the surface of the antenna are very directional. When $t = 0$ and $t = \mathrm{T}/2$, it is obvious that the currents around the gap in the $-45°$ direction are weaker. However, when $t = \mathrm{T}/4$ and $t = 3\mathrm{T}/4$, the currents around the gap in the $-45°$ direction are very strong. For the traditional patch type MED, to realize the 90° phase difference between the equivalent magnetic dipole and the electric dipole depends on the section height of 1/4 wavelength of the short-circuit patch type magnetic dipole antenna. The magnetic dipole of this antenna element applies metallized vias to replace the patch antenna, so a lower profile can be obtained. In addition, the bandwidth of the antenna element can be broadened by adjusting the size of slot in the ground.

Through the electromagnetic software simulation, the variation curves of antenna scattering parameters and gains are obtained as illustrated in Fig. 3(a) and (b), respectively. It can be seen that the common impedance bandwidth of the two ports of the dual-polarized antenna is 40% (3–4.5 GHz, $|S_{11}|$ and $|S_{22}| < -10$ dB), and the isolation of the two polarized ports is generally very high. The isolation at very few high frequencies is not very good, but it can also reach 27 dB. The maximum gain of the antenna is 7.2 dBi, and the fluctuation is very small in the operational frequency band. It is in line with the properties of the MED antenna element and also meets the needs of MIMO antenna applied in base stations.

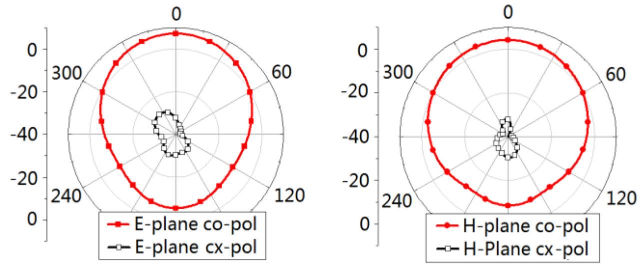

(a) (b)

Fig. 4. Radiation patterns at 3.75 GHz when the antenna element is excited at port 1. (a) Copolarization and cross polarization of E-plane. (b) Copolarization and cross polarization of H-plane.

TABLE II
COMPARISONS OF SOME DUAL-POLARIZED MED ANTENNA ELEMENT

Ref.	Bandwidth (%)	Isolation (dB)	Dimension (λ_0^3)
[2]	24.9	>29	0.82×0.82×0.15
[12]	65.9	>36	1.28×1.28×0.23
[13]	68	>36	1.3×1.3×0.24
[14]	42.5	>24	0.69×0.69×0.13
[15]	20	>35	0.9×0.9×0.28
[16]	50	>17.8	0.8×0.8×0.2
This letter	40	>27	0.58×0.58×0.1

Fig. 4 shows the radiation patterns at the frequency of 3.75 GHz when port 1 is excited. Because the structure of the dual-polarized dielectric integrated MED antenna element is symmetrical, the radiation results generated by feeding port 2 are also symmetrical with the results by feeding port 1. It can be observed that the radiation generated by the antenna is mainly in the 0° direction, and the maximum gain is 7.2 dBi at this time. The cross-polarization discrimination (XPD) of the antenna in the main radiation direction is greater than 37 dB, and the antenna still maintains a relatively high XPD within the radiation coverage range of ±60°. In addition, the front-to-back ratio of the antenna is 14.6 dB.

Table II exhibits comparisons of the relevant parameters of the proposed antenna element in this letter and some dual-polarized MED antenna elements in the existing literatures.

Compared with the common MED antennas, the proposed MED antenna element has a lower profile of 0.1λ. Meanwhile, it has a broad impedance bandwidth of 40% and a high ports isolation of 27 dB.

III. Dual-Polarized MED MIMO Antenna

Four ±45° dual-polarized dielectric integrated MED antenna elements are applied to form a four-element MIMO antenna, as depicted in Fig. 5. Number the four-element dual-polarized MIMO antenna from left to right as elements 1–4, respectively. The MIMO antenna feeding ports are numbered as ports 1–8, respectively, as shown in Fig. 5(b). The MIMO antenna is simulated, fabricated, and measured. The picture of the fabricated antenna is exhibited in Fig. 6. The scattering parameters and radiation characteristics of the MIMO antenna are measured in a microwave anechoic chamber.

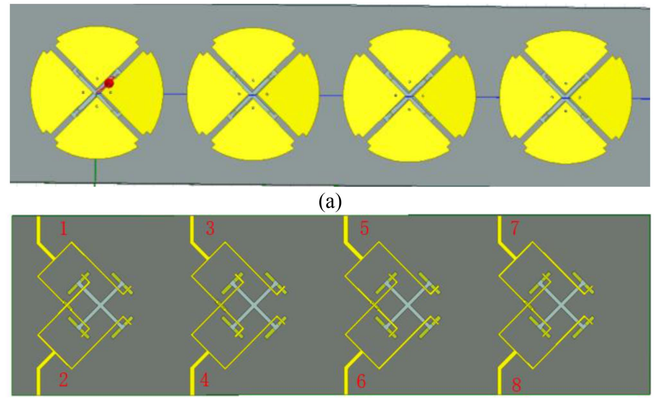

(a) (b)

Fig. 5. Geometry of the MIMO antenna. (a) Top view. (b) Back and detail views of the feeding structure.

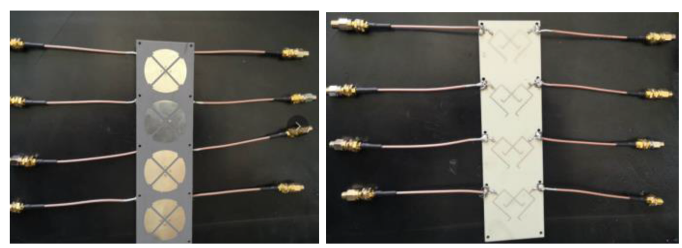

(a) (b)

Fig. 6. Prototype of the fabricated MIMO antenna. (a) Top view. (b) Back view.

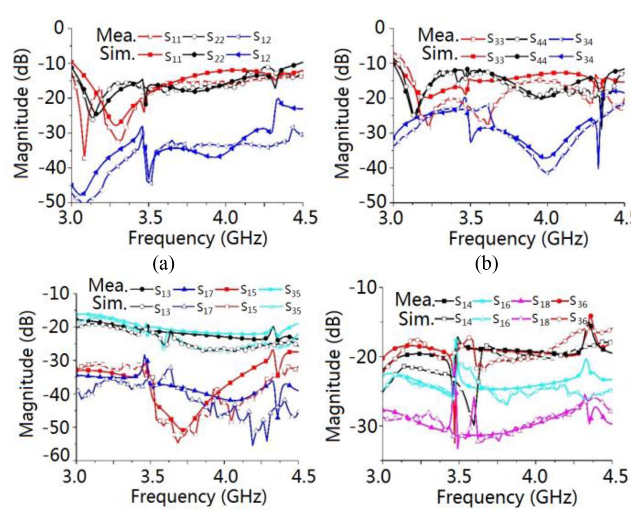

(a) (b) (c) (d)

Fig. 7. Parts of simulated and measured results of scattering parameters of the MIMO antenna. (a) S_{11}, S_{22}, S_{12}. (b) S_{33}, S_{44}, S_{34}. (c) $S_{13}, S_{17}, S_{15}, S_{35}$. (d) $S_{14}, S_{16}, S_{18}, S_{36}$.

As shown in Fig. 7, due to the symmetry of the antenna structure and the large number of ports, other parameters of the MIMO antenna ports can be obtained only by selecting the simulated and measured results of ports 1–4 for comparison.

It can be seen that though there is a certain range of errors in fabrication and measurement, the variation trends of the

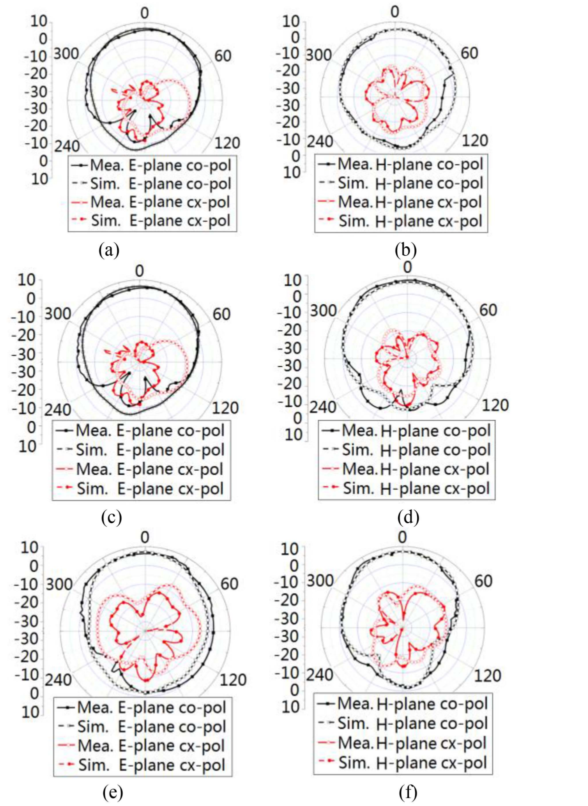

Fig. 8. Simulated and measured radiation patterns of the fabricated MIMO antenna at different frequencies of port 1. (a) E-plane at 3 GHz. (b) H-plane at 3 GHz. (c) E-plane at 3.7 GHz. (d) H-plane at 3.7 GHz. (e) E-plane at 4.5 GHz. (f) H-plane at 4.5 GHz.

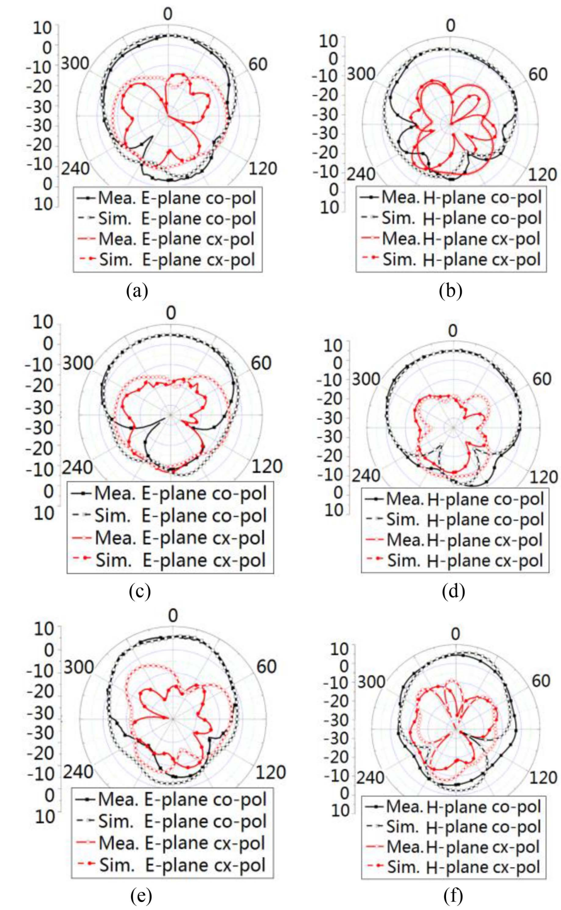

Fig. 9. Simulated and measured radiation patterns of the fabricated MIMO antenna at different frequencies of port 3. (a) E-plane at 3 GHz. (b) H-plane at 3 GHz. (c) E-plane at 3.7 GHz. (d) H-plane at 3.7 GHz. (e) E-plane at 4.5 GHz. (f) H-plane at 4.5 GHz.

measured and simulated scattering coefficients are basically the same and the antenna can achieve good matching and isolation. However, there is still a certain resonant frequency shift and resonant depth difference. The simulated and measured results of antenna elements 1 and 2 are basically consistent, and the antenna has structural symmetry, indicating that the MIMO antenna works normally. The simulated and measured results of the transmission coefficients of other ports are also in good agreement, which verifies the correctness of the design. As can be seen from Fig. 7, each port of the MIMO antenna covers the operational frequency band of 3–4.5 GHz. In this band, as observed in Fig. 7(c) and (d), the isolation of the co-polarization ports (S_{13} and S_{35}) is greater than 16 dB, and the isolation of the orthogonal polarization ports (S_{14} and S_{36}) is greater than 15 dB. It means that the isolations between two adjacent elements are greater than 15 dB.

As illustrated in Figs. 8 and 9, the simulated and measured patterns of ports 1 and 3 at different frequencies are given, respectively. It can be seen that the variation trend of the measured radiation pattern in the range of $\pm 60°$ is also basically the same as that of the simulated results. In the meantime, the antenna can achieve a higher XPD. However, the cross-polarization level of port 3 in Fig. 9 is higher than that of port 1 in Fig. 8. This is because element 2 is located in the middle of the MIMO antenna, which makes the mutual coupling between elements strong, resulting in poor XPD. Therefore, to improve the XPD, it is necessary to increase the isolation between elements. The mutual coupling can be reduced by adding some isolation structures, such as metal strips, SIW columns, or decoupling networks between adjacent elements. In addition, the measured radiation efficiency of the antenna is greater than 70%. The fluctuation trend of the gain in the entire operational frequency band is consistent with the simulated results, which verifies the correctness of the design.

In general, the simulated and measured results of the MIMO antenna scattering parameters are consistent. Furthermore, the simulated and measured results of the antenna radiation pattern are also in good agreement in the upper half space. Because of the existence of the anechoic turntable and the fixed objects in the lower half space, the amplitude of the measured results is lower than the simulated results.

IV. Conclusion

In this letter, a four-element broad low-profile dual-polarized substrate integrated MED MIMO antenna has been proposed. Based on multilayer dielectric integration and microstrip slot coupling feeding technologies, the proposed antenna has achieved a low profile of 0.1λ and a broad impedance bandwidth of 40%. Meanwhile, the characteristics of high ports isolation and high XPD have been realized. The proposed dual-polarized MED MIMO antenna can be used in wireless communication systems.

REFERENCES

[1] K. M. Luk and H. Wong, "A new wideband unidirectional antenna element," *Int. J. Microw. Opt. Technol.*, vol. 1, no. 1, pp. 35–44, Jun. 2006.

[2] L. Siu, H. Wong, and K.-M. Luk, "A dual-polarized magneto-electric dipole with dielectric loading," *IEEE Trans. Antennas Propag.*, vol. 57, no. 3, pp. 616–623, Mar. 2009.

[3] L. Ge and K. M. Luk, "A low-profile magneto-electric dipole antenna," *IEEE Trans. Antennas Propag.*, vol. 60, no. 4, pp. 1684–1689, Apr. 2012.

[4] L. Ge and K. M. Luk, "A magneto-electric dipole antenna with low-profile and simple structure," *IEEE Antennas Wireless Propag. Lett.*, vol. 12, pp. 140–142, 2013.

[5] B. Feng, J. Lai, Q. Zeng, and K. L. Chung, "A dual-wideband and high gain magneto-electric dipole antenna and its 3D MIMO system with metasurface for 5G/WiMAX/WLAN/X-band applications," *IEEE Access*, vol. 6, pp. 33387–33398, 2018.

[6] Y. Li and K.-M. Luk, "60-GHz dual-polarized two-dimensional switch-beam wideband antenna array of aperture-coupled magneto-electric dipoles," *IEEE Trans. Antennas Propag.*, vol. 64, no. 2, pp. 554–563, Feb. 2016.

[7] J. Xu, W. Hong, Z. H. Jiang, and H. Zhang, "Millimeter-wave broadband substrate integrated magneto-electric dipole arrays with corporate low-profile microstrip feeding structures," *IEEE Trans. Antennas Propag.*, vol. 68, no. 10, pp. 7056–7067, Oct. 2020.

[8] J. Xu, W. Hong, Z. H. Jiang, and H. Zhang, "Low-cost millimeter-wave circularly polarized planar integrated magneto-electric dipole and its arrays with low-profile feeding structures," *IEEE Antennas Wireless Propag. Lett.*, vol. 19, no. 8, pp. 1400–1404, Aug. 2020.

[9] Y. Ji, L. Ge, J. Wang, Q. Chen, and W. Wu, "Differentially-fed aperture-coupled magneto-electric dipole antenna with continuously variable beamwidth," *IEEE Open J. Antennas Propag.*, vol. 1, pp. 165–174, 2020.

[10] Y. Tian, J. Ouyang, P. F. Hu, and Y. Pan, "Millimeter-wave wideband circularly polarized endfire planar magneto-electric dipole antenna based on substrate integrated waveguide," *IEEE Antennas Wireless Propag. Lett.*, vol. 21, no. 1, pp. 49–53, Jan. 2022.

[11] H. W. Lai and H. Wong, "Substrate integrated magneto-electric dipole antenna for 5G Wi-Fi," *IEEE Trans. Antennas Propag.*, vol. 63, no. 2, pp. 870–874, Feb. 2015.

[12] B. Q. Wu and K.-M. Luk, "A broadband dual-polarized magneto-electric dipole antenna with simple feeds," *IEEE Antennas Wireless Propag. Lett.*, vol. 8, pp. 60–63, 2009.

[13] Q. Xue, S. W. Liao, and J. H. Xu, "A differentially-driven dual-polarized magneto-electric dipole antenna," *IEEE Trans. Antennas Propag.*, vol. 61, no. 1, pp. 425–430, Jan. 2013.

[14] Y. Li, C. Wang, and Y. X. Guo, "A Ka-band wideband dual-polarized magneto-electric dipole antenna array on LTCC," *IEEE Trans. Antennas Propag.*, vol. 68, no. 6, pp. 4985–4990, Jun. 2020.

[15] N. Ashraf, A. R. Sebak, and A. A. Kishk, "Packaged microstrip line feed network on a single surface for dual-polarized $2N\times 2M$ ME dipole antenna array," *IEEE Trans. Antennas Propag.*, vol. 19, no. 4, pp. 596–600, Apr. 2020.

[16] X. Dai and K. M. Luk, "A wideband dual-polarized antenna for millimeter-wave applications," *IEEE Trans. Antennas Propag.*, vol. 69, no. 4, pp. 2380–2385, Apr. 2021.